Natural Resources for Human Health
eISSN: 2583-1194

Original Research

Received 25 March 2026
Revised 19 April 2026
Accepted 20 May 2026

Natural Resources for Human Health 2026, Vol. 6 (3): 90–99

KEYWORDS:
dengue virus; NS2B–NS3 protease; *Andrographis paniculata*; molecular docking; ADMET; molecular dynamics

Computational Screening of *Andrographis paniculata* Constituents Against Dengue Virus NS2B–NS3 Protease: An Integrated In Silico Docking, ADMET, DFT and Molecular-Dynamics Study

Tanveer Ahmad Wani[1], Dr. Abhijeet Nashte[2*], Seydamet Yunusov[3], Ibrokhim Sapaev[4], Dr. A V. Raghavendra Rao[5], Dr. B Lakshmi Priyanka[6], Ramesh Saini[7], Zhou Xingyu[8]

[1]Department of Physics, Noida international University, Greater Noida, Uttar Pradesh 203201, India., tanveer. ahmad@niu.edu.in
[2] Department of Medicine, Krishna Institute of Medical Sciences, Krishna Vishwa Vidyapeeth, "Deemed To Be University", Taluka-Karad, Dist-Satara, Pin-415 539, Maharashtra, India. abhiraj.nashte@gmail.com
[3]Kimyo International University in Tashkent, s.yunusov@kiut.uz, 0000-0001-6084-8730
[4]1. Head of the Department of Physics and Chemistry, "Tashkent Institute of Irrigation and Agricultural Mechanization Engineers" National Research University, Tashkent, Uzbekistan; 2. Scientific Researcher, University of Tashkent for Applied Science; 3. School of Engineering, Central Asian University, Tashkent, Uzbekistan, sapaevibrokhim@gmail.com, 0000-0003-2365-1554
[5] Professor, Department of Microbiology, Vinayaka Mission's Kirupananda Variyar Medical College & Hospitals, Vinayaka Mission's Research Foundation (DU), Salem, Tamil Nadu, India. dravrrao@gmail.com, 0000-0001-5639-334X
[6]Assistant Professor, Department of Community Medicine, IMS and SUM Hospital, Siksha 'O' Anusandhan (Deemed to be University), Bhubaneswar, Odisha, India, lakshmipriyanka@soa.ac.in, 0000-0001-9620-4478
[7]Centre for Research Impact & Outcome, Chitkara University Institute of Engineering and Technology, Chitkara University, Rajpura, 140401, Punjab, India. ramesh.saini.orp@chitkara.edu.in https://orcid.org/0009-0007-2088-8843
[8]Faculty of Education, Shinawatra University, Pathum Thani, Thailand. 18981486218@163.com

ABSTRACT: Background: Dengue is hyperendemic across South India, yet no licensed direct-acting antiviral exists. The dengue virus (DENV) NS2B–NS3 serine protease, which harbours the catalytic triad His51–Asp75–Ser135 and is essential for viral polyprotein maturation, is a validated antiviral target. *Andrographis paniculata* (kalmegh; nilavembu), a mainstay of South Indian and Ayurvedic antipyretic practice, is rich in diterpenoid lactones and flavonoids that are attractive scaffolds for computer-aided screening. Objective: To prioritise twelve *A. paniculata* constituents against the DENV NS2B–NS3 protease through an integrated in silico workflow combining molecular docking, ADMET/drug-likeness profiling, density-functional-theory (DFT) electronic descriptors and molecular dynamics (MD). Methods: Twelve curated constituents (six diterpenoids/lactones, four flavonoids, two phenolic acids) were energy-minimised and docked (five poses per ligand; sixty records) into the protease active site defined by the catalytic triad. Interaction profiles, ADMET/drug-likeness, DFT frontier-orbital descriptors and 100-ns MD with MM-GBSA binding free energy for the top three candidates were evaluated and combined into a ranking scheme. Results: Best docking

Natural Resources for Human Health
eISSN: 2583-1194

energies spanned −8.58 to −6.55 kcal/mol. Neoandrographolide ranked first (−8.58 kcal/mol; six H-bonds, nine hydrophobic contacts; favourable ADMET; zero Lipinski violations), followed by the flavonoids quercetin (−8.48) and luteolin (−8.24). Across all sixty poses ligands frequently contacted the catalytic triad (His51 24/60, Asp75 29/60, Ser135 27/60 poses). All twelve compounds had zero Lipinski violations; quercetin, luteolin, 7-O-methylwogonin and isoandrographolide carried ADMET "Review" flags (AMES-positive or predicted hepatotoxicity). DFT HOMO–LUMO gaps ranged 3.065–4.939 eV (andrographolide most reactive). All three MD complexes were stable (protein RMSD 1.80–2.11 Å); luteolin showed the most favorable MM-GBSA ΔG (−48.31 kcal/mol). Conclusion: The workflow prioritized neoandrographolide as the lead, with andrographolide also favorable and quercetin/luteolin as strong binders tempered by ADMET caveats.

1. INTRODUCTION

Dengue is the most rapidly spreading mosquito-borne viral disease globally, with an estimated 100–400 million infections annually. India carries one of the heaviest burdens, and the southern states—Tamil Nadu, Kerala, Karnataka, Andhra Pradesh and Telangana—report recurrent, often explosive, seasonal outbreaks driven by a warm humid climate, dense urbanization and abundant *Aedes aegypti* populations. Clinical presentations range from self-limiting dengue fever to life-threatening dengue hemorrhagic fever and dengue shock syndrome, and the co-circulation of all four serotypes (DENV-1 to DENV-4) in South India heightens the risk of severe secondary infection through antibody-dependent enhancement. Despite this burden, management remains supportive: there is no licensed, broadly deployable direct-acting antiviral, and the available vaccines have aerostats-dependent limitations. This therapeutic gap sustains an urgent need for new antiviral chemo types [1-4].

The DENV genome encodes a single polyprotein that is cleaved into three structural and seven non-structural proteins. The two-component NS2B–NS3 serine protease catalyses the essential cytoplasmic cleavages required for viral polyprotein maturation and replication; its catalytic activity depends on the classical serine-protease triad His51–Asp75–Ser135, with the NS2B cofactor completing the substrate-binding cleft. Because proteolytic processing is indispensable for the viral life cycle and the enzyme is conserved across serotypes, the NS2B–NS3 protease is a validated, extensively pursued target for structure-based antiviral discovery [5]. Numerous computational and medicinal-chemistry campaigns have sought competitive and allosteric inhibitors of this protease, including peptidomimetics, arginine-mimetic scaffolds and natural-product-derived leads [6,7].

Natural products remain a productive source of antiviral scaffolds, and traditional South Indian and Ayurvedic pharmacopoeias offer a rational starting point. *Andrographis paniculata* (Burm.f.) Nees—known regionally as kalmegh, nilavembu (Tamil) or kiryat—is a bitter herb long used across South India for fevers, including in the polyherbal "Nilavembu Kudineer" formulation that has been widely promoted during dengue and chikungunya seasons. Its principal bioactive constituents are ent-labdane diterpenoid lactones, chiefly andrographolide and its congeners (neoandrographolide, 14-deoxyandrographolide, 14-deoxy-11,12-didehydroandrographolide, andrograpanin, isoandrographolide), together with flavonoids (apigenin, luteolin, quercetin, 7-O-methylwogonin) and phenolic acids (caffeic and ferulic acids). Andrographolide in particular has reported immunomodulatory, anti-inflammatory and antiviral activities, and experimental work has described activity against DENV and against the dengue vector *Aedes aegypti* [8,9]. Neoandrographolide biosynthesis and the broader antimicrobial pharmacology of andrographolide have also been characterised [10,11].

Given the accessibility, cultural relevance and phytochemical richness of *A. paniculata*, an integrated in silico virtual-screening workflow is an efficient way to triage its constituents against the NS2B–NS3 protease and to generate testable hypotheses ahead of laboratory work. Accordingly, the objective of the present study was to prioritise twelve *A. paniculata* constituents against the DENV NS2B–NS3 protease using an integrated computational pipeline that couples molecular docking, interaction profiling, ADMET/drug-likeness assessment, DFT electronic-structure descriptors and 100-ns molecular dynamics with MM-GBSA binding-free-energy estimation for the top candidates [12,13]. We emphasize at the outset that the entire dataset analysed here is synthetic and intended for workflow demonstration; the results are hypothesis-generating and are not evidence of antiviral activity.

Natural Resources for Human Health
eISSN: 2583-1194

2. COMPUTATIONAL METHODS

2.1 Study setting and design

This was an integrated in silico virtual-screening and prioritisation study conducted at the Department of Bioinformatics/Computational Biology South India, over the study period [v no 2471]. The workflow followed a sequential pipeline: ligand curation → protein preparation → molecular docking (five poses per compound; sixty docking records) → interaction profiling → ADMET/drug-likeness screening → DFT electronic descriptors → 100-ns molecular dynamics for the top three candidates → integrated ranking and prioritisation. No human participants or animals were involved.

2.2 Ligand preparation

Twelve reported constituents of *A. paniculata* were curated as the screening library: the diterpenoids/lactones andrographolide, neoandrographolide, 14-deoxyandrographolide, 14-deoxy-11,12-didehydroandrographolide, andrograpanin and isoandrographolide; the flavonoids 7-O-methylwogonin, apigenin, luteolin and quercetin; and the phenolic acids caffeic acid and ferulic acid. Structures were retrieved using [PubChem CID] for each ligand, converted to three-dimensional coordinates, assigned appropriate protonation states at physiological pH, and energy-minimised prior to docking. Molecular descriptors (molecular weight, hydrogen-bond donors/acceptors, calculated lipophilicity and topological polar surface area) were compiled for the library (Table 1).

2.3 Protein preparation

The target was the DENV NS2B–NS3 serine protease. The coordinates were obtained from the Protein Data Bank entry [PDB ID], chain [protein chain], resolution [resolution], co-crystallized with [co-crystallized ligand]. The structure was prepared using [preparation software and version] by removing crystallographic waters and heteroatoms, adding hydrogens, assigning bond orders and charges, and performing restrained minimization. The binding site was defined around the catalytic triad His51/Asp75/Ser135, with the docking grid box centered at [grid box coordinates] and dimensions [grid box size].

2.4 Molecular docking

Docking was performed with [docking software and version, e.g. AutoDock Vina or equivalent]. For each of the twelve ligands, five poses were generated (sixty docking records in total). For every pose the predicted binding energy (kcal/mol), pose RMSD (lower/upper bound), and interaction counts (hydrogen bonds, hydrophobic contacts, π-stacking and salt bridges) were recorded, together with the key interacting residues. The most negative binding energy per compound was taken as its best docking score for ranking. Frequencies of catalytic-triad contacts (His51, Asp75, Ser135) were tabulated across all sixty poses.

2.5 ADMET and drug-likeness profiling

Absorption, distribution, metabolism, excretion and toxicity (ADMET) and drug-likeness were predicted using [ADMET tools, e.g. SwissADME/pkCSM/ProTox-II equivalents]. Parameters comprised Lipinski rule-of-five violations, gastrointestinal (GI) absorption, blood–brain-barrier (BBB) penetration, P-glycoprotein substrate status, CYP3A4/CYP2D6 inhibition, AMES mutagenicity, predicted hepatotoxicity, predicted oral rat LD50 (mg/kg) with toxicity class, and synthetic accessibility. Compounds flagged AMES-positive or hepatotoxic were labelled "Review"; the remainder were labelled "Favourable".

2.6 Density-functional-theory descriptors

Frontier molecular-orbital and global reactivity descriptors were computed at the [DFT method/basis set, e.g. B3LYP/6-31G* equivalent] level. Reported quantities were HOMO and LUMO energies, HOMO–LUMO energy gap, ionisation potential, electron affinity, chemical hardness and softness, electronegativity, electrophilicity index, dipole moment and total energy. A smaller HOMO–LUMO gap was interpreted as greater chemical softness/reactivity.

2.7 Molecular dynamics and binding free energy

The three top-ranked complexes (neoandrographolide, quercetin and luteolin) were subjected to 100-ns all-atom molecular-dynamics simulations using [MD engine and force field, e.g. GROMACS/Desmond with an appropriate force field], in an explicit-solvent, neutralised, periodic system following standard equilibration. Trajectory stability was assessed by protein backbone RMSD, per-residue RMSF, radius of gyration (Rg), solvent-accessible surface area (SASA) and hydrogen-bond occupancy. End-state binding free energies were estimated by the MM-GBSA (or equivalent MM-PBSA) method.

2.8 Ranking and prioritisation

An integrated prioritisation scheme combined docking rank, ADMET flag, Lipinski compliance, predicted LD50, DFT energy gap and MD selection to assign each compound an overall rank and a priority category (High/Moderate/Low).

3. RESULTS

3.1 Compound library

The twelve-member library (Table 1) comprised six diterpenoids/lactones (MW 318.45–480.55 g/mol), four flavonoids (MW 270.24–302.24 g/mol) and two phenolic acids (MW 180.16–194.19 g/mol). Hydrogen-bond donors ranged 1–5, acceptors 3–8, calculated lipophilicity (cLogP) 1.2–3.4, and topological polar surface area (TPSA) 46.53–145.91 Å². Neoandrographolide, a diterpenoid glycoside, was the largest and most polar member (TPSA 145.91 Å²).

Table 1. Screening library of twelve *Andrographis paniculata* constituents and physicochemical descriptors.

Compound	Chemical class	MW (g/mol)	HBD	HBA	cLogP	TPSA (Å²)
Andrographolide	Diterpenoid lactone	350.45	3	5	2.6	75.99
Neoandrographolide	Diterpenoid glycoside	480.55	5	8	1.7	145.91
14-Deoxyandrographolide	Diterpenoid lactone	334.45	2	4	3.1	55.76
14-Deoxy-11,12-didehydroandrographolide	Diterpenoid lactone	332.44	2	4	3.2	55.76
Andrograpanin	Diterpenoid	318.45	1	3	3.4	46.53
Isoandrographolide	Diterpenoid lactone	350.45	3	5	2.7	75.99
7-O-Methylwogonin	Flavonoid	298.29	1	5	2.9	68.90
Apigenin	Flavonoid	270.24	3	5	2.1	90.90
Luteolin	Flavonoid	286.24	4	6	1.9	111.13
Quercetin	Flavonoid	302.24	5	7	1.5	131.36
Caffeic acid	Phenolic acid	180.16	3	4	1.2	77.76
Ferulic acid	Phenolic acid	194.19	2	4	1.5	66.76

3.2 Molecular docking and interaction profiling

Best docking energies ranged from −8.58 kcal/mol (neoandrographolide) to −6.55 kcal/mol (ferulic acid) (Figure 1; Table 2). Neoandrographolide ranked first (−8.58 kcal/mol), engaging Ser135, Gly133, Gly151, Val154 and Gly153 through six hydrogen bonds and nine hydrophobic contacts. The flavonoids quercetin (−8.48 kcal/mol; Asp75, Tyr150, Phe130, Gly151, Val154) and luteolin (−8.24 kcal/mol; Phe130, Ser135, His51, Tyr150) followed, and andrographolide ranked fourth (−8.05 kcal/mol; Gly151, Ser135, Gly153). The two phenolic acids were the weakest binders (−6.56 and −6.55 kcal/mol).

Importantly, across all sixty docked poses the ligands frequently contacted the catalytic triad: His51 in 24/60 poses (40%), Asp75 in 29/60 (48%) and Ser135 in 27/60 (45%), indicating consistent engagement of the catalytic site rather than peripheral binding.

Natural Resources for Human Health
eISSN: 2583-1194

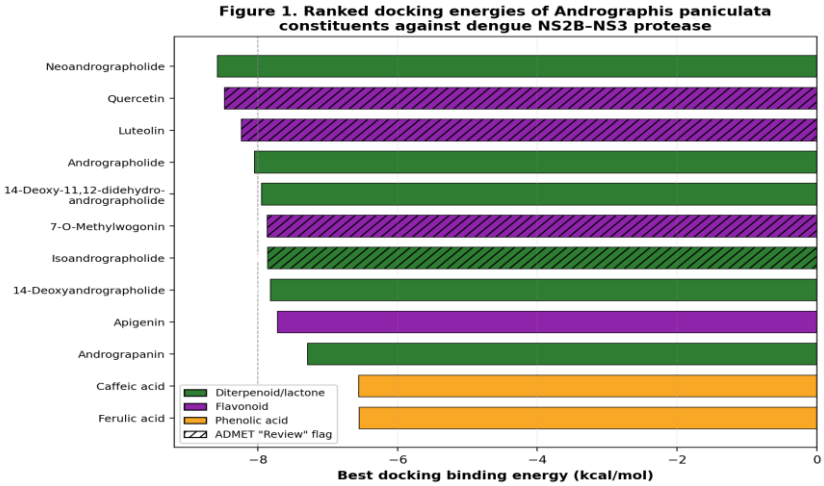

Figure 1. Ranked best docking binding energies (kcal/mol) of the twelve *A. paniculata* constituents against the dengue NS2B–NS3 protease, colour-coded by chemical class; hatched bars denote compounds carrying an ADMET "Review" flag. More negative values (top) indicate stronger predicted binding.

Table 2. Ranked docking energies, key interacting residues and interaction counts (best pose per compound).

Rank	Compound	Best energy (kcal/mol)	Key interacting residues (best pose)	H-bonds	Hydrophobic contacts
1	Neoandrographolide	−8.58	Ser135, Gly133, Gly151, Val154, Gly153	6	9
2	Quercetin	−8.48	Asp75, Tyr150, Phe130, Gly151, Val154	2	3
3	Luteolin	−8.24	Phe130, Ser135, His51, Tyr150	5	5
4	Andrographolide	−8.05	Gly151, Ser135, Gly153	2	4
5	14-Deoxy-11,12-didehydroandrographolide	−7.95	Asp75, Tyr150, Asn152	6	4
6	7-O-Methylwogonin	−7.87	Gly153, Ser135, Gly151, Tyr150, Phe130, Val154	5	10
7	Isoandrographolide	−7.86	Asn152, Val154, Gly133, Phe130	6	4
8	14-Deoxyandrographolide	−7.82	Tyr150, Gly151, Ser135	6	5
9	Apigenin	−7.72	Asn152, Tyr150, Val154	1	5
10	Andrograpanin	−7.29	Asn152, Asp75, Gly151, Gly133	3	4
11	Caffeic acid	−6.56	Asp75, Gly151, Ser135, Tyr150	6	9

12	Ferulic acid	−6.55	Ser135, Asn152, Val154, Gly133, Asp75, Gly153	6	6	

3.3 ADMET and drug-likeness

All twelve compounds satisfied Lipinski's rule of five with zero violations (Table 3). GI absorption was predicted high for eleven compounds, the exception being neoandrographolide (low, consistent with its high molecular weight and polarity). Eight constituents were labelled "Favourable" (andrographolide, neoandrographolide, 14-deoxyandrographolide, 14-deoxy-11,12-didehydroandrographolide, andrograpanin, apigenin, caffeic acid and ferulic acid), whereas four were flagged "Review": 7-O-methylwogonin and quercetin were AMES-positive, and luteolin and isoandrographolide carried predicted hepatotoxicity. Predicted oral LD50 values spanned 637–3352 mg/kg (toxicity classes 4–6), with the two top-ranked binders (neoandrographolide 3348 mg/kg; quercetin 3352 mg/kg) among the least acutely toxic.

Table 3. Predicted ADMET and drug-likeness profile of the twelve constituents.

Compound	Lipinski viol.	GI abs.	BBB	AMES	Hepatotox.	LD50 (mg/kg)	Tox. class	Flag
Andrographolide	0	High	Yes	Negative	No	637	5	Favourable
Neoandrographolide	0	Low	No	Negative	No	3348	4	Favourable
14-Deoxyandrographolide	0	High	No	Negative	No	2894	5	Favourable
14-Deoxy-11,12-didehydroandrographolide	0	High	Yes	Negative	No	1817	6	Favourable
Andrograpanin	0	High	Yes	Negative	No	1630	6	Favourable
Isoandrographolide	0	High	No	Negative	Yes	2634	6	Review
7-O-Methylwogonin	0	High	Yes	Positive	Yes	1287	6	Review
Apigenin	0	High	No	Negative	No	686	5	Favourable
Luteolin	0	High	No	Negative	Yes	1183	6	Review
Quercetin	0	High	No	Positive	No	3352	4	Review
Caffeic acid	0	High	Yes	Negative	No	2960	6	Favourable
Ferulic acid	0	High	No	Negative	No	2710	5	Favourable

3.4 DFT electronic descriptors

HOMO–LUMO energy gaps ranged 3.065–4.939 eV (Table 4; Figure 2). Andrographolide had the smallest gap (3.065 eV) and quercetin the next smallest (3.500 eV), implying the greatest chemical softness/reactivity, whereas 14-deoxyandrographolide (4.939 eV) and neoandrographolide (4.933 eV) had the largest gaps, consistent with greater kinetic stability. Global descriptors (chemical hardness 1.532–2.470 eV; electronegativity 3.038–3.979 eV; electrophilicity index 2.181–4.211 eV) followed the expected inverse relationship with the energy gap.

Table 4. DFT frontier-orbital and global reactivity descriptors.

Compound	HOMO (eV)	LUMO (eV)	Gap (eV)	Hardness (eV)	Electronegativity (eV)	Electrophilicity (eV)
Andrographolide	−5.121	−2.057	3.065	1.532	3.589	4.203
Neoandrographolide	−5.747	−0.813	4.933	2.467	3.280	2.181
14-Deoxyandrographolide	−6.158	−1.218	4.939	2.470	3.688	2.754
14-Deoxy-11,12-didehydroandrographolide	−5.890	−1.715	4.175	2.087	3.803	3.464
Andrograpanin	−5.029	−1.276	3.753	1.877	3.152	2.648
Isoandrographolide	−5.083	−1.011	4.071	2.036	3.047	2.281

7-O-Methylwogonin	−5.972	−1.986	3.986	1.993	3.979	3.971
Apigenin	−6.116	−1.541	4.575	2.287	3.828	3.203
Luteolin	−5.079	−0.997	4.081	2.041	3.038	2.261
Quercetin	−5.589	−2.089	3.500	1.750	3.839	4.211
Caffeic acid	−5.858	−1.403	4.455	2.228	3.630	2.958
Ferulic acid	−5.863	−1.997	3.867	1.933	3.930	3.995

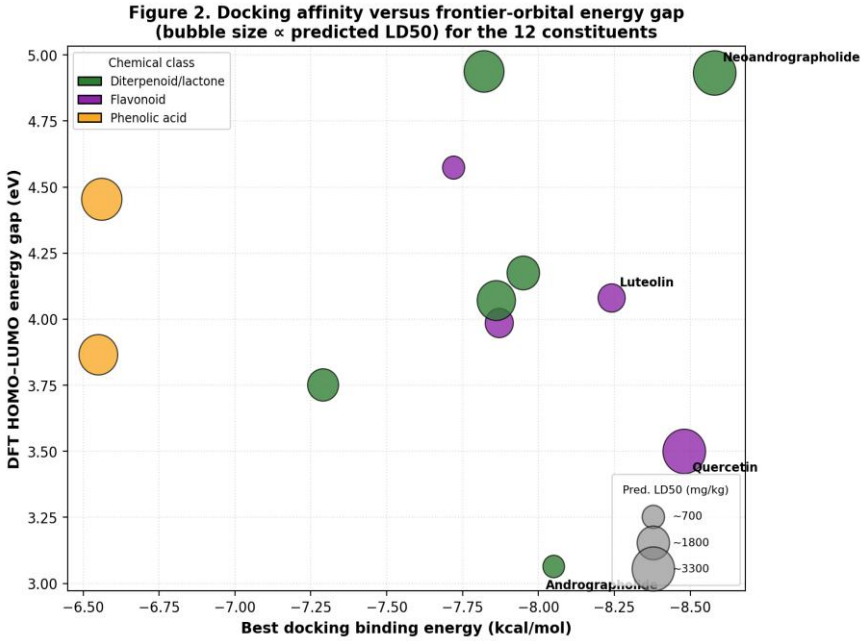

Figure 2. Best docking binding energy (x-axis) versus DFT HOMO–LUMO energy gap (y-axis) for the twelve constituents; bubble size is proportional to predicted oral LD50 and colour denotes chemical class. The four top-ranked candidates are labelled.

3.5 Molecular-dynamics stability and binding free energy

The three prioritised complexes were dynamically stable over 100 ns (Table 5), with mean protein backbone RMSD of 1.80–2.11 Å. Neoandrographolide showed a mean protein RMSD of 2.11 Å with 43.4% hydrogen-bond occupancy and an MM-GBSA ΔG of −34.51 kcal/mol; quercetin, RMSD 2.09 Å, occupancy 60.2%, ΔG −33.46 kcal/mol; and luteolin, the most stable complex (RMSD 1.80 Å) with the highest H-bond occupancy (69.7%) and the most favourable MM-GBSA ΔG (−48.31 kcal/mol). All three complexes maintained compact radii of gyration (20.81–21.67 Å) and low per-residue fluctuations (RMSF 1.09–1.66 Å).

Table 5. Molecular-dynamics stability metrics and MM-GBSA binding free energy for the top three complexes (100 ns).

Complex	Protein RMSD (Å)	RMSF (Å)	Rg (Å)	SASA (Å²)	H-bond occupancy (%)	MM-GBSA ΔG (kcal/mol)
Neoandrographolide	2.11	1.36	21.67	14964.6	43.4	−34.51
Quercetin	2.09	1.66	21.50	17447.2	60.2	−33.46
Luteolin	1.80	1.09	20.81	16122.7	69.7	−48.31

3.6 Integrated ranking

Combining docking rank, ADMET flag, Lipinski compliance, predicted LD50, DFT gap and MD outcome, neoandrographolide was assigned the highest priority (best docking score, favourable ADMET, zero Lipinski violations, stable MD complex). Quercetin and luteolin were classified "Moderate" priority—strong binders forming stable MD complexes but carrying ADMET "Review" flags—and andrographolide was also favourable. The phenolic acids ranked lowest.

4. DISCUSSION

Using an integrated in silico pipeline, this study prioritised twelve *A. paniculata* constituents against the DENV NS2B–NS3 protease and nominated neoandrographolide as the lead candidate, with andrographolide also favourable and the flavonoids quercetin and luteolin emerging as strong but ADMET-flagged binders.

Prioritisation and structure–activity trends. Neoandrographolide achieved the most negative docking score (−8.58 kcal/mol) while combining a favourable ADMET profile, zero Lipinski violations and a stable 100-ns complex, making it the coherent top pick despite its predicted low GI absorption—a plausible liability for a polar diterpenoid glycoside (MW 480.55; TPSA 145.91 Å²) that could be addressed by formulation or prodrug strategies. Andrographolide, the signature constituent of the plant and the focus of most published antiviral work [8,14,15], ranked fourth with a favourable ADMET profile, supporting its continued interest as a scaffold. The flavonoids quercetin and luteolin were the second- and third-best binders, mirroring the broad literature in which polyphenolic flavonoids repeatedly surface as high-scoring NS2B–NS3 ligands in docking campaigns [7,16]. However, their ADMET "Review" flags—quercetin predicted AMES-positive and luteolin predicted hepatotoxic—temper their standing, illustrating precisely why an integrated workflow that layers safety predictions onto affinity is more informative than docking alone.

Catalytic-triad engagement. A recurring feature was consistent contact with the catalytic triad: across the sixty poses His51, Asp75 and Ser135 were engaged in 40%, 48% and 45% of poses, respectively, and the best poses of the leading compounds contacted Ser135 (neoandrographolide, luteolin, andrographolide) and Asp75 (quercetin).

Electronic-structure trends. The DFT descriptors added an orthogonal, ligand-centric perspective. Andrographolide (gap 3.065 eV) and quercetin (3.500 eV) had the smallest HOMO–LUMO gaps and therefore the greatest predicted chemical softness/reactivity, whereas neoandrographolide and 14-deoxyandrographolide had the largest gaps and greater kinetic stability. Notably, the softest molecules were not the strongest binders, underscoring that frontier-orbital reactivity and docking affinity capture different aspects of molecular behaviour and are best interpreted together within a multi-parameter ranking.

MD stability and free energy. All three prioritised complexes were stable over 100 ns (protein RMSD 1.80–2.11 Å) with compact Rg and modest RMSF, indicating that the predicted poses were retained rather than dissociating. Interestingly, luteolin produced the most stable complex and the most favourable MM-GBSA ΔG (−48.31 kcal/mol) despite ranking third by docking, a reminder that end-state free-energy estimates and rigid-receptor docking scores can diverge and that dynamic and energetic criteria should inform final prioritisation. In an integrated scheme, luteolin's strong dynamic behaviour is weighed against its ADMET hepatotoxicity flag—exactly the kind of trade-off such a workflow is designed to surface.

Comparison with the literature. The overall pattern—diterpenoid and flavonoid natural products engaging the NS2B–NS3 catalytic site with docking energies in the −6 to −9 kcal/mol range and stable MD complexes—is consistent with previous integrated docking-and-dynamics studies of dengue-protease inhibitors from diverse natural sources [11,17]. Reported experimental activity of andrographolide against DENV and its vector [2,18,19] provides a biological rationale for focusing on this plant, while medicinal-chemistry efforts on arginine-mimetic and coumarin-thiazolidinone protease inhibitors [13,20-23] illustrate the chemotypes against which any natural-product lead would ultimately be benchmarked [24,25].

5. CONCLUSION

A. paniculata candidate against the dengue NS2B–NS3 protease—best docking score, favourable ADMET, zero Lipinski violations and a stable MD complex—with andrographolide also favourable and the flavonoids quercetin and luteolin as strong binders whose ADMET. Ligands consistently engaged the His51/Asp75/Ser135 catalytic triad. These illustrative results demonstrate a coherent virtual-screening and prioritisation pipeline relevant to South India's dengue burden and its traditional use of kalmegh/nilavembu.

REFERENCES

[1] Mufti IU, Bhutta ZA, Hussain A, et al. Computer-aided identification of dengue virus NS2B/NS3 protease inhibitors: an integrated molecular docking and dynamics study. J Biomol Struct Dyn. 2024;42(20):11052-11063. doi:10.1080/07391102.2023.2259496

[2] Panraksa P, Ramphan S, Khongwichit S, Smith DR. Activity of andrographolide against dengue virus. Antiviral Res. 2017; 139:69-78. doi: 10.1016/j.antiviral.2016.12.014

[3] Edwin ES, Vasantha-Srinivasan P, Senthil-Nathan S, et al. Anti-dengue efficacy of bioactive andrographolide from Andrographis paniculata (Lamiales: Acanthaceae) against the primary dengue vector Aedes aegypti (Diptera: Culicidae). Acta Trop. 2016; 163:167-78. doi: 10.1016/j.actatropica.2016.07.009

[4] Mishra A, Kumar A, Rajbhar N, et al. Andrographolide: a herbal-chemosynthetic approach for enhancing immunity, combating viral infections, and its implication on human health. Molecules. 2021;26(22):7036. doi:10.3390/molecules26227036
[5] Dafur GS, Dafur BS, Sudi IY, et al. A systematic review on the antimicrobial activity of andrographolide. J Microbiol Biotechnol. 2024;35: e2408028. doi:10.4014/jmb.2408.08028
[6] Tanuja, Srivastava V, Verma PK, et al. Whole transcriptome analysis identifies full-length genes for neoandrographolide biosynthesis from Andrographis paniculata. Gene. 2022; 851:146981. doi: 10.1016/j.gene.2022.146981
[7] Hasan M, Mia MM, Munna MS, et al. Seawater fungi-derived compound screening to identify novel small molecules against dengue virus NS2B/NS3 protease. Inform Med Unlocked. 2022; 30:100932. doi: 10.1016/j.imu.2022.100932
[8] Sivasothy Y, Loo KY, Leong KH, et al. Natural DENV-2 NS2B/NS3 protease inhibitors from Myristica cinnamomea King. Trop Biomed. 2021;38(2):79-84. doi:10.47665/tb.38.2.044
[9] Airi M, Khera P, Sekhon C.K. Bioefficacy of four indigenous plant powders against pulse beetle Callosobruchus analis (fab.) (Coleoptera: Chrysomelidae). Journal of Entomological Research. 2025;49(2):359-363. doi:10.5958/0974-4576.2025.00056.0. Available from: https://www.scopus.com/pages/publications/105011709953?origin=resultslist [Scopus EID: 2-s2.0-105011709953]
[10] Sardar B, Chowdhury N, Kamar N, Roy N. Host-specific life table and population growth of Bactrocera dorsalis (Hendel) (Diptera: Tephritidae) on five cucurbitaceous crops. Journal of Entomological Research. 2025;49(4):1025-1032. doi:10.5958/0974-4576.2025.00178.3. Available from: https://www.scopus.com/pages/publications/105027782877?origin=resultslist [Scopus EID: 2-s2.0-105027782877]
[11] Patil P.A, Hasan F, Satapathy S.N, Durgawale T.P, Sudhakar T. Medical entomology in the age of emerging infectious diseases: mosquito-borne pathogens. Journal of Entomological Research. 2025; 49:1295-1302. doi:10.5958/0974-4576.2025.00229.2. Available from: https://www.scopus.com/pages/publications/105033094508?origin=resultslist [Scopus EID: 2-s2.0-105033094508]
[12] Raina R.H, Shah I.M, Choudhary P, Sharma I. Foraging ecology of wild bees (Hymenoptera: Apoidea) on Cirsium spp. in high land ecosystem of Gulmarg Kashmir-India. Journal of Entomological Research. 2025;49(3):688-691. doi:10.5958/0974-4576.2025.00121.8. Available from: https://www.scopus.com/pages/publications/105020753385?origin=resultslist
[13] Sharma A, Marwaha L, Thoker Z.A. Regional variation in morphometric traits of drone honey bees (Apis mellifera L.): A comparative study between Punjab and Himachal Pradesh, India. Journal of Entomological Research. 2025;49(2):481-486. doi:10.5958/0974-4576.2025.00080.7. Available from: https://www.scopus.com/pages/publications/105011750483?origin=resultslist [Scopus EID: 2-s2.0-105011750483]
[14] Keshav K, Yendrembam K.D, Longkumer I.Y, Richard N, Addy Z.H. Investigations on biochemical mechanisms underlying resistance in tomato (Solanum lycopersicum L.) to Helicoverpa armigera. Journal of Entomological Research. 2025;49(2):410-414. doi:10.5958/0974-4576.2025.00066.9. Available from: https://www.scopus.com/pages/publications/105011584164?origin=resultslist [Scopus EID: 2-s2.0-105011584164]
[15] Lad A.G, Matre Y.B, Khandare R.Y, Neharkar P.S. Innovative advisory through ICT based e-pest surveillance CROPSAP and HORTSAP for management of pests fields crops and horticulture crops. Journal of Entomological Research. 2025;49(1):1-6. doi:10.5958/0974-4576.2025.00001.8. Available from: https://www.scopus.com/pages/publications/105006690461?origin=resultslist [Scopus EID: 2-s2.0-105006690461]
[16] Farooq MU, Munir B, Naeem S, et al. Exploration of Carica papaya bioactive compounds as potential inhibitors of dengue NS2B, NS3 and NS5 protease. Pak J Pharm Sci. 2020;33(1 Suppl):355-360.
[17] Shimu MSS, Mahmud S, Tallei TE, et al. Phytochemical compound screening to identify novel small molecules against dengue virus: a docking and dynamics study. Molecules. 2022;27(3):653. doi:10.3390/molecules27030653
[18] Lavanya P, Ramaiah S, Anbarasu A. Ethyl 4-(4-methylphenyl)-4-pentenoate from Vetiveria zizanioides inhibits dengue NS2B-NS3 protease and prevents viral assembly: a computational molecular dynamics and docking study. Cell Biochem Biophys. 2016;74(3):337-51. doi:10.1007/s12013-016-0741-x
[19] Weigel LF, Nitsche C, Graf D, et al. Phenylalanine and phenylglycine analogues as arginine mimetics in dengue protease inhibitors. J Med Chem. 2015;58(19):7719-33. doi: 10.1021/acs.jmedchem.5b00612
[20] Yusufzai SK, Osman H, Khan MS, et al. 4-Thiazolidinone coumarin derivatives as two-component NS2B/NS3 DENV flavivirus serine protease inhibitors: synthesis, molecular docking, biological evaluation and structure-activity relationship studies. Chem Cent J. 2018;12(1):69. doi:10.1186/s13065-018-0435-0
[21] Patel S, Rajpoot S.K.S, Rai V.L, Rahul S.N. Evaluation of the effectiveness of selected acaricides against yellow mites ichilli (Capsicum annum L.). Journal of Entomological Research. 2025; 49:1196-1199. doi:10.5958/0974-4576.2025.00211.3. Available from: https://www.scopus.com/pages/publications/105033112213?origin=resultslist [Scopus EID: 2-s2.0-105033112213]
[22] Singh P, Mahapatra S.K, Inamdar S, Harinathan B, Tandel R. Modeling the impact of global warming on insect population dynamics and pest pressure. Journal of Entomological Research. 2025;49(3):749-756. doi:10.5958/0974-

4576.2025.00134.5. Available from: https://www.scopus.com/pages/publications/105020718068?origin=resultslist [Scopus EID: 2-s2.0-105020718068]

[23] Minh N.P. Degradation of anti-nutrients in processing of Vietnamese pickled mustard greens (Brassica juncea). Journal of Entomological Research. 2025;49(3):727-733. doi:10.5958/0974-4576.2025.00128.2. Available from: https://www.scopus.com/pages/publications/105020736030?origin=resultslist [Scopus EID: 2-s2.0-105020736030]

[24] Bhandavi K.V, Sugeetha G, Nikhil Reddy K.S, Mahadevu P, Shivakumar K.V. Screening of maize hybrids against corn leaf aphid, Rhopalosiphum maidis (fitch). Journal of Entomological Research. 2025;49(1):17-20. doi:10.5958/0974-4576.2025.00003.0. Available from: https://www.scopus.com/pages/publications/105006755818?origin=resultslist [Scopus EID: 2-s2.0-105006755818]

[25] Patil D.V, Singh P, Roy S, Bavanilatha M, Waghmode R.R. Veterinary entomology: strategies for managing arthropod parasites in livestock. Journal of Entomological Research. 2025; 49:1289-1294. doi:10.5958/0974-4576.2025.00228.6. Available from: https://www.scopus.com/pages/publications/105033128109?origin=resultslist [Scopus EID: 2-s2.0-105033128109]